

September 29, 2016

PREPARED FOR SUBMISSION TO JHEP

The Excitation of the Global Symmetry-Breaking Vacuum in Composite Higgs Models

Sylvain Fichet ^a, Gero von Gersdorff ^b, Eduardo Pontón ^a and Rogerio Rosenfeld ^a

^a *ICTP South American Institute for Fundamental Research & Instituto de Física Teórica
Universidade Estadual Paulista, São Paulo, Brazil*

^b *Departamento de Física, Pontifícia Universidade Católica de Rio de Janeiro, Rio de Janeiro,
Brazil*

E-mail: sylvain.fichet@gmail.com, gersdorff@gmail.com,
eponton@ift.unesp.br, rosenfel@ift.unesp.br

ABSTRACT: We consider scenarios of Higgs compositeness where the Higgs doublet arises as a pseudo-Nambu Goldstone boson. Our focus is the physical scalar (“radial”) excitation associated with the global symmetry breaking vacuum, which we call the *global Higgs*. For the minimal case of a $SO(5)/SO(4)$ coset, the couplings of the global Higgs to Standard Model (SM) particles are fully determined by group theoretical factors and two decay constants. The global Higgs also couples to the composite resonances of the theory, inducing an interaction with the SM gauge bosons at one-loop. We thoroughly analyze representative fermionic sectors, considering a global Higgs both in the **5** and **14** representations of $SO(5)$ and taking into account the renormalization group evolution of couplings in the composite sector. We derive the one-loop effective couplings and all decays of the global Higgs, showing that its decay width over mass can range from $\mathcal{O}(10^{-3})$ to $\mathcal{O}(1)$. Because of the multiplicity of the resonances, the coupling of the global Higgs to gluons is sizeable, potentially opening a new window into composite models at the LHC.

Contents

1	Introduction	1
2	A Global Higgs-like Scalar in the Composite Higgs Paradigm	3
3	Bosonic Couplings	7
3.1	Self-Couplings	7
3.2	Couplings to the Goldstone Bosons and Vector Resonances	7
4	Fermionic Couplings	9
4.1	A Simple Top Sector	9
4.2	Other Embeddings and Light Quarks	10
4.3	Benchmark Models	13
5	Effective One-loop Couplings to the SM Gauge Bosons	14
6	Running Couplings in the Composite Sector	16
7	Decays	19
7.1	Case I: Closed Decay Channels into Fermion Resonances	20
7.2	Case II: Open Decay Channels into Fermion Resonances	22
8	Conclusions	23
A	The Global Higgs in the 14 Representation of $SO(5)$	24
B	Yukawa Structures	26
C	Loop Functions	26

1 Introduction

It is by now established with a high degree of significance that the 125 GeV resonance discovered at the LHC in July 2012 is an excitation of the broken electroweak vacuum. This discovery sheds light on the nature of electroweak symmetry breaking (EWSB), and is consistent with an elementary Higgs doublet as posed in the Standard Model of Particle Physics (SM).

Now that it is clear that a scalar field is present at the TeV scale, it becomes more urgent to understand why the scale of electroweak breaking is so small compared to ultra-violet (UV) scales such as the Planck mass, M_{Pl} . A first approach to tackle this hierarchy problem is to assume that new particles appear near the electroweak scale in order to cancel

the huge $O(M_{\text{Pl}}^2)$ corrections that tend to destabilize the weak scale. A second possibility is to assume that this scalar field exists only at low energies, as a bound state of more fundamental constituents. At energies higher than the compositeness scale Λ , the EW scalar would dissolve into constituents of spin higher than zero, which can be immune to large quadratic corrections.

This second possibility, that interprets the Higgs boson as a composite object, is at the center of our attention in this work. The fact that we have tested the Higgs boson with energies comparable to its mass without revealing any obvious substructure, so that the binding energy must be comparable to its rest mass, suggests that the bound state arises from some underlying strong dynamics, as opposed to being a weakly bound state. The generic scenario of strong dynamics leading to a composite scalar field is, however, in tension with the observed properties of the Higgs boson. Indeed, one would generically expect that such a composite field would feature a broad decay width, and be accompanied by other, nearby resonances. However, the Higgs boson is observed to be narrow, and no other light states (e.g. vectorlike fermions or additional spin-1 fields) have been observed up to now at the LHC.

A class of scenarios that naturally reconciles strong coupling dynamics with the observed Higgs boson is the one postulating that the EW scalar doublet is actually the pseudo-Nambu-Goldstone boson (pNGB) of a global symmetry G spontaneously broken to a subgroup G' at an energy scale \hat{f} . A small explicit breaking of G would then be at the origin of the EW scalar potential, perhaps allowing for a dynamical understanding of EWSB itself. In this framework, a mass gap automatically splits the EW scalar from heavier resonances, and its couplings are naturally weak so that the Higgs boson has a narrow width. These scenarios are referred to as “pNGB composite Higgs” models (for a recent review, see [1]). The magnitude of \hat{f} is bounded from below by LHC searches for e.g. vectorlike fermions, as well as from deviation from the expected SM Higgs couplings. The magnitude of the compositeness scale Λ can also be bounded from below using Higgs coupling measurements.

Although composite Higgs models usually assume an underlying strongly-coupled dynamics, their UV completion has received relatively little attention. Instead, most of the literature focuses on the low-energy effective theory describing the Higgs boson properties below the compositeness scale. More precisely, the standard way to proceed is to work within the non-linear σ -model of the G/G' coset. This effective description is fully appropriate at low energies, when the G' vacuum remains unperturbed. In contrast, whenever the G' vacuum can be excited, the corresponding degrees of freedom must be included in the σ -model. This implies that a particle with the quantum numbers of the vacuum, *i.e.* a new neutral, CP-even scalar is potentially present in the effective field theory. We shall refer to this scalar as the *global Higgs* throughout the rest of this paper, and denote it by ϕ . The mass m_ϕ of the global Higgs should be smaller than the cutoff of the effective theory, but apart from that it is a free parameter.

In this paper, we will investigate the conditions under which the global Higgs can arise and what are its properties. The possible presence of a global Higgs in the composite Higgs framework seems rather intriguing, and to the best of our knowledge, has so far only been

studied in Refs. [2, 3]. We will go beyond the simple models studied in [2, 3] by including couplings to spin-1 resonances, and also study more general fermion sectors as well as the possibility of embedding the global Higgs into non-minimal $SO(5)$ representations. Moreover, we formulate the theory entirely in terms of the nonlinear variables, allowing for a more direct comparison to the usual literature on composite Higgs models.

In Section 2, we establish a broad picture of the global Higgs properties based on general arguments. Focusing on the $SO(5)/SO(4)$ coset, we derive the bosonic couplings of the global Higgs in Sec. 3. We then define a set of benchmark scenarios for the fermionic sector in Sec. 4, and compute systematically the 1-loop effective couplings of the global Higgs to SM gauge bosons in Sec. 5. The renormalized couplings of the composite sector are computed in Sec. 6, and the decay widths and branching fractions are presented in Sec. 7. Section 8 contains our conclusions.

2 A Global Higgs-like Scalar in the Composite Higgs Paradigm

Composite Higgs models – where the EW symmetry is broken by the condensation of pseudo-NGB’s arising from the spontaneous breaking of an approximate global symmetry at a higher scale – are typically studied in the low energy regime, below the scale of global symmetry breaking. As such, one needs only to parametrize the pNGB degrees of freedom, thereby implementing the global symmetry non-linearly. Presumably, such a low-energy description is obtained by integrating out heavy modes. These heavy states include the global Higgs, scalar radial modes that, together with the pNGB’s, would enter in a complete G multiplet (denoted by Φ) and would allow a linear implementation of the full global symmetry (not just of the unbroken subgroup G').

An interesting example is provided by the model considered in Ref. [4]. In that case, the breaking of the global symmetry is induced by 4-fermion interactions with a coefficient near criticality. Indeed, allowing for a mild tuning of this coefficient so that it lies slightly above a certain critical value, the symmetry breaking mechanism can be equivalently described by the condensation of a (composite) scalar in a complete G -representation,¹ such that there is a hierarchy between the symmetry breaking scale, \hat{f} , and the cutoff Λ associated with the non-renormalizable 4-fermion interactions. The global Higgs typically has a mass m_ϕ of the order of the symmetry breaking scale. Interestingly, some fermion resonances are expected to have masses of order m_ϕ or somewhat below.² On the other hand, as explained in [4], spin-1 resonances associated with the underlying strong dynamics are expected to be heavier, with masses of order Λ .

¹In the model studied in [4], the G -symmetry was $SO(5)$, and the scalar was in the fundamental of $SO(5)$. After condensation, the symmetry is broken to $G' = SO(4)$, generating 4 (p)NGB’s plus one real scalar, the global Higgs. In other non-minimal examples one can have both additional pNGB’s, as well as additional massive scalar degrees of freedom. One such example is the breaking of $SO(5)$ by the **14** representation, which in addition to the massive $SO(4)$ singlet “radial” mode, has an additional massive symmetric tensor of $SO(4)$ in its spectrum.

²As in models of top condensation [5, 6], there is a definite relation between the global Higgs mass and the dynamical mass of the fermions that bind together to form the global Higgs.

Thus, one can be in a situation where some of the fermionic resonances, in addition to the global Higgs, may be more readily accessible than other higher spin excitations. The collider phenomenology of such fermion states has been widely studied in the context of general composite Higgs scenarios [7–13] and beyond [14–18]. Here our focus is rather on the properties of the global Higgs.

We start by establishing a picture of the global Higgs properties in general terms, leaving a more concrete presentation to the following section. First of all, since the global Higgs is by definition an excitation of the G/G' vacuum, it interacts with the pNGBs that parameterize this vacuum. Due to the approximate shift symmetry, such interactions involve covariant derivatives, and one expects tree-level couplings of the global Higgs to the pNGB's, *i.e.* to the SM Higgs boson and to the longitudinal components of the electroweak gauge bosons. The global Higgs could also in principle couple to the vector resonances of the strongly interacting sector. These couplings introduce another scale in the model, which we call f_ρ , and will be discussed in the following section.

Importantly the global Higgs has couplings to the fermions in the spectrum and also, via loop effects, to pairs of gluons and photons. In order to discuss such effects it will be useful to summarize first the framework of partial compositeness [19], which allows to elegantly accommodate the SM flavor structure within the composite Higgs paradigm. One assumes here the presence of an elementary sector, in addition to the composite sector giving rise to the Higgs and other resonances. The elementary sector contains three families of chiral fermions q, u, d, l, e ,³ and mimics exactly, in its $SU(2)_L \times U(1)_Y$ quantum numbers, the fermion field content of the SM. The composite sector, on the other hand, consists of vector-like states in complete G representations. Each $SU(2)_L$ multiplet in the elementary sector is associated with a composite G -multiplet Q, U, D, L, E , which itself contains some states with the corresponding $SU(2)_L \times U(1)_Y$ quantum numbers. This allows bilinear mixing between the elementary and composite sectors, thereby breaking explicitly the global symmetry G .⁴ In this framework, the light mass eigenstates are identified with the SM fermions. They are accompanied by heavy vectorlike “partners”.

The vectorlike masses of the composite fermion sector will be denoted by M_Q, M_U, M_D, M_L and M_E . The composite fermions also have interactions with the pNGB's, which will eventually give rise to the SM Yukawa couplings. One therefore often refers to the Yukawa interactions between the composite states as “proto-Yukawa” interactions. Having embedded the pNGBs into the G -multiplet Φ , proto-Yukawa interactions take the schematic form⁵

$$\mathcal{L}_{\text{proto-Y}} = -\xi_U \mathcal{O}_U(\Phi) \bar{Q} U - \xi_D \mathcal{O}_D(\Phi) \bar{Q} D - \xi_E \mathcal{O}_E(\Phi) \bar{L} E + \text{h.c.} , \quad (2.1)$$

where the $\mathcal{O}_X(\Phi)$ are appropriate functions of Φ such that the above terms are G invariant.

³Generation indices are not shown.

⁴Another source of explicit G -breaking is the gauging of $SU(2)_L \times U(1)_Y$ itself.

⁵Note that we are being rather schematic since the precise contractions between the various fields depend on the G -representations they belong to. For our present purposes this will be sufficient (specific examples will be shown in the following section).

The elementary-composite mixing terms take the form

$$\mathcal{L}_{\text{mix}} = -\Delta_q \bar{Q} \cdot q - \Delta_u \bar{U} \cdot u - \Delta_d \bar{D} \cdot d - \Delta_l \bar{L} \cdot l - \Delta_e \bar{E} \cdot e + \text{h.c.} , \quad (2.2)$$

where the dot denotes an appropriate projection of the states in the G -multiplets with the correct SM quantum numbers. The physical SM states are linear combinations of the elementary and composite states with mixing angles controlled by the mixing masses $\Delta_q, \dots, \Delta_e$. Only through the bilinear mixing above do the lightest mass eigenstates acquire interactions with the pNGB's contained in Φ , thus leading to Yukawa terms as in the SM.⁶

A scenario that has received much attention – commonly known as *anarchy* – assumes that the proto-Yukawa couplings $\xi_{U,D,E}$ are all of the same order (and of order one to a few). The observed hierarchies in the SM fermion spectrum then arise from hierarchies in the mixing angles above: the lightest fermions are mostly elementary and hence weakly coupled to the SM Higgs field (the pNGB states in Φ), while the heavy top has a sizeable component in the composite sector (*i.e.* the mixing angle is large). A second, perhaps less well-motivated, possibility is that the mixing angles are of the same order, and instead the SM fermion mass hierarchies arise from hierarchies in the proto-Yukawa couplings themselves. We will consider both possibilities.

Let us now turn to the couplings of the global Higgs to the fermion sector. First, since the global Higgs is contained in Φ , it couples to composite fermion pairs as dictated by the proto-Yukawa structures of Eq. (2.1). We can thus expect a coupling of the global Higgs to the heavy mass eigenstates, controlled by the $SO(5)$ Yukawa couplings $\xi_{U,D,E}$. The global Higgs can also couple to a SM fermion and one of its vectorlike partners. Such couplings require the mixing terms of Eq. (2.2). However, the proto-Yukawa interactions induce couplings between the global Higgs and SM fermion pairs only after EWSB. The reason is that the global Higgs is, by definition, a SM singlet and there are no fermion bilinear singlets in the SM. The induced couplings will be seen to be proportional to the SM fermion mass.

As already mentioned, there are loop-level induced interactions between the global Higgs and gluons or photons. Although suppressed, these can play a central role in the global Higgs phenomenology. These couplings are induced in complete analogy to the SM case, through loops of colored or charged states whose masses get a contribution from the breaking of the global symmetry. The importance of such effects depends on the size of the proto-Yukawa couplings and therefore on whether we assume an anarchic scenario or not.⁷ The point is that the composite fermion masses can receive both symmetry breaking ($\sim \xi \hat{f}$) and symmetry preserving contributions. As is well known, whenever the vector-like

⁶The vectorlike masses, Yukawa couplings and mixing parameters need not be simultaneously diagonal in flavor space but, for simplicity, this is not reflected in our notation above.

⁷Note that, since Eq. (2.1) is G -symmetric, no such couplings between gluons/photons and the SM Higgs are induced at this point, since here the SM Higgs is an exact NGB. Only the global Higgs enters into the above discussion. When the mixing angles of Eq. (2.2) are taken into account, couplings between the SM Higgs and gluons/photons are induced. The contribution from the elementary sector is dominated by the top quark, as in the SM. The contributions from the composite sector, on the other hand, are suppressed by their large vector-like masses. The deviations from the SM couplings in such scenarios have been studied elsewhere (see, e.g. [12]) and are not the focus of our study.

mass is small compared to the symmetry breaking contribution, the loop-induced coupling of the global Higgs to two gauge bosons (through a triangle diagram) exhibits a non-decoupling behavior that is already apparent when the Yukawa coupling ξ is of order one. This behavior remains qualitatively true when the vector-like mass is comparable to the symmetry breaking one. Therefore, whenever the vector-like masses M_Q, \dots, M_E are not much larger than $\xi \hat{f}$, each resonance gives a comparable contribution, and the net effect can be encoded into an effective multiplicity factor. In the first scenario discussed above, with order one to a few proto-Yukawa couplings and hierarchical mixing angles, one can therefore expect that the heavy sector associated with each SM state can give a sizeable effect. The details depend on the G -representations of the spin-1/2 resonances, which may be different for the up-quark sector, the down-quark sector and the leptons. Also, if one insists to remain in the perturbative regime at the scale of the global Higgs mass, a large number of resonances can put an upper bound on the Yukawa couplings ξ , so that the symmetry-breaking effects cannot be arbitrarily large compared to the vectorlike effects. We defer further details to the next section. However, to get an idea of the size of the multiplicity factors involved, one can consider what would have been the situation if the SM Yukawa couplings were all of order one. In that case, for the gluon fusion process, for instance, one would have obtained an amplitude about 6 times larger than the top contribution, a factor that gets squared in the cross section. The multiplicity factors in the global Higgs case can potentially be even larger since the global symmetry structure often suggests the presence of relatively large representations, as we will see in the next section. It is therefore important to analyze such enhancements in more detail.

On the opposite extreme, *i.e.* the case where the mixing angles are all of order one but the proto-Yukawa couplings are hierarchical, one expects that only the resonances associated with the top sector will be important. The resonances associated with the lighter fermions will give contributions to the loop processes that are suppressed, much as those of the light fermions in the SM Higgs case. Hence, this limit provides a “minimum” contribution to the 1-loop amplitudes, and thus we will present it as one of the benchmarks in our study, regardless of how likely it is to be realized in nature.

In summary, the picture that emerges is that the physical excitation of the global symmetry breaking vacuum, the global Higgs, can be amongst the lightest states of a strongly-coupled UV completion of composite Higgs scenarios. It should couple to the Higgs and longitudinal electroweak gauge bosons at tree-level, and to the SM fermions proportionally to their masses. In addition, the global Higgs interacts at 1-loop with the SM gauge bosons via loops of the (possibly many) fermion resonances. This last feature is dependent on the realization of the fermion sector. The production of the global Higgs and its study may thus shed some light on the UV completion of composite Higgs models. In the next sections we explore in more detail the expected properties of the global Higgs in specific scenarios.

3 Bosonic Couplings

We turn now to the detailed properties of the global Higgs, starting with its dominant tree-level interactions to bosons, which are rather model independent. The fermion sector will be discussed subsequently. To be definite we will focus on the case where $G = SO(5)$ and $G' = SO(4) = SU(2)_L \times SU(2)_R$. Here, weak isospin is identified with $SU(2)_L$, while hypercharge is embedded as $Y = T_R^3$ of $SU(2)_R$.⁸

In order to describe the vacuum fluctuations of the $SO(5)/SO(4)$ sigma-model, the $SO(5)/SO(4)$ NGBs need to be embedded into a $SO(5)$ representation. We choose to embed them into the fundamental **5** of $SO(5)$,⁹ by defining a scalar Φ parametrized as

$$\Phi = U_5 \mathcal{H}, \quad (3.1)$$

where U_5 is the $SO(5)/SO(4)$ NGB matrix and \mathcal{H} the remaining “radial” degree of freedom. The vev of \mathcal{H} will be denoted by $\hat{f}e_5$, where e_5 denotes a unit vector in the radial direction. The fluctuation ϕ of \mathcal{H} around its vev, given by

$$\mathcal{H} = (\hat{f} + \phi)e_5, \quad (3.2)$$

is the global Higgs.

3.1 Self-Couplings

Having introduced the $SO(4)$ singlet degree of freedom \mathcal{H} , a non-trivial potential $V(\mathcal{H})$ is needed to stabilize it at the non-zero vev $\langle \mathcal{H} \rangle = \hat{f} \neq 0$ that breaks the global symmetry down to $SO(4)$. The potential for \mathcal{H} is in principle arbitrary, the only requirements being $\frac{d}{d\mathcal{H}} V(\mathcal{H})|_{\mathcal{H}=\hat{f}} = 0$, $\frac{d^2}{d\mathcal{H}^2} V(\mathcal{H})|_{\mathcal{H}=\hat{f}} > 0$. As the global Higgs self-interactions are irrelevant for low-energy phenomenology, it is enough to consider the expansion of $V(\mathcal{H})$ up to quartic order,

$$V(\mathcal{H}) = \frac{1}{4}\lambda \left(\mathcal{H}^2 - \hat{f}^2 \right)^2. \quad (3.3)$$

With this parametrization, the λ parameter corresponds to the quartic coupling of the global Higgs, and the global Higgs mass is given by

$$m_\phi = \sqrt{2\lambda}\hat{f}. \quad (3.4)$$

3.2 Couplings to the Goldstone Bosons and Vector Resonances

Although we have argued above that the spin-1 resonances may be amongst the heaviest new physics states (and are therefore not the focus of this work), their presence can still leave an imprint in the properties of the global Higgs, which results in an additional free parameter f_ρ . We therefore present the bosonic sector, that consists of \mathcal{H} , the pNGB's in Φ (*i.e.* the SM Higgs doublet) and a complete spin-1 multiplet of $SO(5)$ (in the adjoint

⁸There is also a $U(1)_X$ factor, such that hypercharge is actually $Y = T_R^3 + X$. Only fermions carry non-zero X charge, see Tab. 1.

⁹We present in App. A the embedding into a symmetric traceless **14** of $SO(5)$.

representation), in addition to the elementary gauge bosons that give rise to the SM gauge boson sector.

Quite generically, the global Higgs couples to the pNGB states in Φ and to the various spin-1 states. These couplings follow from the bosonic Lagrangian (see, e.g. [20])

$$\begin{aligned} \mathcal{L}_{\text{bos}} = & \frac{1}{2}(\nabla_\mu \mathcal{H})^2 - V(\mathcal{H}) + \frac{1}{4}f_\rho^2 \left(\mathcal{A}_\mu^A - i[U_5^\dagger D_\mu U_5]^A \right)^2 \\ & - \frac{1}{4g_\rho^2}(\mathcal{F}_{\mu\nu}^A)^2 - \frac{1}{4g_0^2}(w_{\mu\nu}^a)^2 - \frac{1}{4g_0'^2}(b_{\mu\nu})^2, \end{aligned} \quad (3.5)$$

where the covariant derivative D_μ contains the elementary gauge fields w_μ and b_μ only. The heavy spin-1 resonances are denoted by \mathcal{A}_μ^A , including both $SO(4)$ ($A = a$) and $SO(5)/SO(4)$ ($A = \hat{a}$) resonances. We have used the following definitions

$$U_5 = \exp \left(\frac{\sqrt{2}i}{f} h^{\hat{a}} T^{\hat{a}} \right), \quad \nabla_\mu \mathcal{H} = \left(\partial_\mu - i \mathcal{A}_\mu^{\hat{a}} T^{\hat{a}} \right) \mathcal{H}. \quad (3.6)$$

In Ref. [4] it was shown that this Lagrangian can be obtained from a theory of 4-fermion interactions. As already pointed out there, \mathcal{L}_{bos} is in fact more general, as it is recognized to correspond to a 2-site model Lagrangian where the radial mode of the $SO(5) \rightarrow SO(4)$ breaking of the second site is included. Therefore, the couplings of ϕ should be fairly general and applicable to a wide class of UV completions of models considered in the literature.

Notice that when $f_\rho \rightarrow \infty$, which sets $\mathcal{A}_\mu^A = i[U_5^\dagger D_\mu U_5]^A$, one can rewrite the theory as a *linear* sigma model in terms of the fiveplet $\Phi = U_5 \mathcal{H}$. For finite f_ρ , the couplings of \mathcal{H} to the pNGB's deviate from those of the linear sigma model due to the mixing with the coset spin-1 resonances. In order to diagonalize this mixing, we focus on the terms quadratic in the pNGB's $h^{\hat{a}}$ and the coset resonances $\mathcal{A}^{\hat{a}}$. We get

$$\begin{aligned} & \frac{1}{2}|\nabla \mathcal{H}|^2 + \frac{1}{4}f_\rho^2 \left(\mathcal{A}_\mu^A - i[U_5^\dagger D_\mu U_5]^A \right)^2 \\ & = \frac{1}{2}(\partial_\mu \phi)^2 + \frac{1}{4}(\hat{f} + \phi)^2 (\mathcal{A}_\mu^{\hat{a}})^2 + \frac{f_\rho^2}{4} \left(\mathcal{A}_\mu^{\hat{a}} + \frac{\sqrt{2}}{f} D_\mu h^{\hat{a}} \right)^2 + \dots \end{aligned} \quad (3.7)$$

To disentangle the Goldstones and the vector bosons, define the shifted field \mathcal{B}_μ and choose f according to

$$\mathcal{A}_\mu = \mathcal{B}_\mu - \frac{\sqrt{2}f}{\hat{f}^2} D_\mu h, \quad f^{-2} = \hat{f}^{-2} + f_\rho^{-2}, \quad (3.8)$$

which eliminates the cross term $D_\mu h^{\hat{a}} \mathcal{A}_\mu^{\hat{a}}$ and renders the pNGB kinetic term canonical:

$$\mathcal{L} = \frac{1}{2}(\partial_\mu \phi)^2 + \frac{1}{2}(D_\mu h^{\hat{a}})^2 + \frac{m_a^2}{2}(\mathcal{B}_\mu^{\hat{a}})^2 + \left(\frac{1}{2}\hat{f}\phi + \frac{1}{4}\phi^2 \right) \left(\mathcal{B}_\mu^{\hat{a}} - \frac{\sqrt{2}f}{\hat{f}^2} D_\mu h^{\hat{a}} \right)^2. \quad (3.9)$$

The last term contains all the interactions. In particular one has the following interaction linear in ϕ :

$$\mathcal{L} \supset \frac{f^2}{\hat{f}^3} \phi (D_\mu h^{\hat{a}})^2 \equiv f_H^{-1} \mathcal{O}_H, \quad (3.10)$$

with $\mathcal{O}_H = \frac{1}{2}\phi(D_\mu h^{\hat{a}})^2 = \phi|D_\mu H|^2$, where $H = \frac{1}{\sqrt{2}}(h^{\hat{2}} + ih^{\hat{1}}, h^{\hat{4}} - ih^{\hat{3}})^T$ is the SM Higgs doublet. We therefore identify the induced coefficient for this dimension-5 interaction as $f_H^{-1} = 2r_v \hat{f}^{-1}$, with

$$r_v \equiv \frac{f^2}{\hat{f}^2} = \frac{f_\rho^2}{f_\rho^2 + \hat{f}^2} = \frac{m_\rho^2}{m_a^2} \leq 1. \quad (3.11)$$

Here we have identified the mass of the spin-1 $SO(4)$ resonances \mathcal{A}_μ^a , given by $m_\rho^2 = \frac{1}{2}g_\rho^2 f_\rho^2$, and of the $SO(5)/SO(4)$ resonances $\mathcal{B}_\mu^{\hat{a}}$, given by $m_a^2 = \frac{1}{2}g_\rho^2(f_\rho^2 + \hat{f}^2)$.

The linear sigma model result $f_H^{-1} = 2\hat{f}^{-1}$ is indeed recovered in the limit $f_\rho \rightarrow \infty$. For finite f_ρ , however, the scale suppressing the interaction in Eq. (3.10) can differ by order one from both the naive decay constant \hat{f} which appears in other interactions (see the next section), as well as from the Higgs decay constant, f , which controls the couplings of the pNGB Higgs. As we can see, f_H sets the coupling of a single global Higgs to both a pair of SM Higgses, as well as to pairs of W's and Z's through their longitudinal polarizations, i.e., couplings of the form $m_V^2 f_H^{-1} \phi V_\mu V^\mu$.

One notices that couplings of the global Higgs to transversely polarized SM gauge bosons are absent at this level (they are suppressed by a loop factor or, after including EWSB effects, by $\mathcal{O}(v^2/f_H^2)$). However, they are crucial for phenomenological studies and will be addressed later.

4 Fermionic Couplings

The couplings of the global Higgs to the fermions in the theory are more model dependent. First, one should notice that in the previous section we considered the simplest possibility where there exists a single global Higgs that, together with the four pNGB's that constitute the SM Higgs doublet, falls into a 5 of $SO(5)$. It may be possible, however, that the pNGB's arise from larger $SO(5)$ representations. Connected to this, there is significant model-building freedom to choose the G -multiplets for the fermionic resonances, the only constraint being that they contain a subset of states with the appropriate SM quantum numbers to allow mixing and the implementation of the partial compositeness paradigm.

We will therefore be content with describing some illustrative possibilities and settle on a few representative benchmark scenarios, that could be used for further phenomenological studies. In order to set up the framework, we will start by focusing on a simple top sector. We will then comment on possible variations and on the corresponding constructions necessary for the lighter generations (more precisely, the differences between the up-quark, down-quark and lepton sectors).

4.1 A Simple Top Sector

We are interested in the coupling of ϕ to fermion pairs which arises from the $SO(5)$ symmetric Yukawa couplings, as in Eq. (2.1). We will first consider a minimal top-sector, consisting of vector-like top-partners F and S , which transform in the $\mathbf{5}_2$ and $\mathbf{1}_2$ of the $SO(5) \times U(1)_X$ group respectively. In addition, we include two elementary fields q_L^{el} and t_R^{el}

with the usual SM quantum numbers. The $SO(5)$ Higgs, Φ , will be assumed to transform in the fundamental of $SO(5)$, as in the previous subsection. We can therefore write the Yukawa coupling [4]

$$\mathcal{L}_{\xi_t} = -\xi_t \Phi^i (\bar{F}_L^i S_R + \text{h.c.}) , \quad (4.1)$$

where $\Phi = U_5 (\hat{f} + \phi) e_5$. One can immediately verify that the $SO(4)$ four-plet arising from F does not acquire Yukawa couplings to ϕ before EWSB. We can therefore focus on the $SU(2)_L$ singlet sector which consists of two left-handed fields, (F_L^5, S_L) as well as three right-handed fields (F_R^5, S_R, t_R^{el}) . Under the SM, these fields are $SU(2)$ singlets with hypercharge $\frac{2}{3}$, *i.e.* they transform like the right handed top quark. There will thus be in general one mixing angle in the left-handed sector and three in the right-handed one. We will simplify the discussion by decoupling one vectorlike state [for instance (S_L, t_R^{el}) or (S_L, F_R^5)], so that one is left with only one mixing angle $s_{t_R} = \sin \alpha_{t_R}$, that rotates the remaining two right-handed fields to the mass eigenbasis T_R, t_R . The Lagrangian of the hypercharge $\frac{2}{3}$ top states then reads

$$\mathcal{L}_{1\frac{2}{3}} = -m_T \bar{T}_L T_R - \xi_t \phi (c_{t_R} \bar{T}_L T_R + s_{t_R} \bar{T}_L t_R) + \text{h.c.} \quad (4.2)$$

with $m_T = \xi_t \hat{f} / c_{t_R}$ and t_R denotes the physical right-handed top quark. Note that neglecting electroweak breaking, the physical top-quark does not possess Yukawa coupling to ϕ , only a “mixed” one involving also the heavy top resonance.

After electroweak symmetry breaking, the physical top quark acquires also a Yukawa coupling to ϕ , which is universally given by

$$\mathcal{L}_{\phi t \bar{t}} = -\frac{m_t}{\hat{f}} \phi \bar{t} t . \quad (4.3)$$

In the following we will neglect EWSB effects, since they are a small perturbation for the physics at \hat{f} .

4.2 Other Embeddings and Light Quarks

The above choice of top partners is by no means unique. There exist many choices for the representations of the top (and other fermion) partners. As already stated, the paradigm of partial compositeness simply requires that all SM fermions appear in these representations at least once (such that mixing with the elementary states can take place), and that at least one of each kind appear in the $SO(5)$ -invariant Yukawa couplings. The typical representations considered in the literature (see, e.g. [12]) are the **1**, **5**, **10** or **14** of $SO(5)$. They will be denoted by S , F , A , B respectively. Their decompositions are detailed in Table 1.

Instead of working out in detail other possible top sectors, we will move on to describe various possibilities that can also be applied to the composite states that partner with the light SM fermions. We start by noticing that not all combinations of fermion partners allow for simple renormalizable Yukawa couplings with the $SO(5)$ breaking field in the fundamental. For instance, choosing two quark partners F and F' , one either needs to

$SO(5) \times U(1)_X$	$SO(4) \times U(1)_X$	$SU(2)_L \times U(1)_Y$
$1_{\frac{2}{3}}$	$1_{\frac{2}{3}}$	$1_{\frac{2}{3}}$
$5_{\frac{2}{3}}$	$1_{\frac{2}{3}} + 4_{\frac{2}{3}}$	$1_{\frac{2}{3}} + (2_{\frac{1}{6}} + 2_{\frac{7}{6}})$
$5_{-\frac{1}{3}}$	$1_{-\frac{1}{3}} + 4_{-\frac{1}{3}}$	$1_{-\frac{1}{3}} + (2_{-\frac{5}{6}} + 2_{\frac{1}{6}})$
5_{-1}	$1_{-1} + 4_{-1}$	$1_{-1} + (2_{-\frac{3}{2}} + 2_{\frac{1}{2}})$
$10_{\frac{2}{3}}$	$4_{\frac{2}{3}} + 6_{\frac{2}{3}}$	$(2_{\frac{1}{6}} + 2_{\frac{7}{6}}) + (1_{-\frac{1}{3}} + 1_{\frac{2}{3}} + 1_{\frac{5}{3}} + 3_{\frac{2}{3}})$
$14_{\frac{2}{3}}$	$1_{\frac{2}{3}} + 4_{\frac{2}{3}} + 9_{\frac{2}{3}}$	$1_{\frac{2}{3}} + (2_{\frac{1}{6}} + 2_{\frac{7}{6}}) + (3_{-\frac{1}{3}} + 3_{\frac{2}{3}} + 3_{\frac{5}{3}})$

Table 1. Decomposition of the smallest $SO(5) \times U(1)_X$ representations under both the custodial $SO(4)$ and the SM $SU(2)_L \times U(1)_Y$.

resort to a $SO(5)$ breaking field in the **14**, or to nonrenormalizable Yukawa couplings:

$$\mathcal{L}_\xi^{\dim 4} = -\xi \bar{F}^i \Psi_{ij} F'^j, \quad \text{or} \quad \mathcal{L}_\xi^{\dim 5} = -\frac{\xi}{\hat{f}} \bar{F}^i \Phi^i F'^j \Phi^j. \quad (4.4)$$

In the case that the pNGB's arise from a **14**, we define the global Higgs as the mode in the $SO(4)$ singlet direction $\frac{1}{\sqrt{20}} \text{diag}(1, 1, 1, 1, -4)$. The two choices above lead to different couplings between ϕ and the various $SO(4)$ representations. The possible $SO(4)$ representations from the decompositions in Table 1 are the **1**, **4**, **6**, and **9** and are assumed to be canonically normalized. We denote them by s , f , a and b , respectively. The $SO(5)$ symmetric proto-Yukawa couplings induce Yukawa interactions with the global Higgs, e.g.

$$\bar{F} \Psi F' = \frac{2}{\sqrt{5}} \phi \bar{s} s' + \frac{1}{2\sqrt{5}} \phi \bar{f} f'. \quad (4.5)$$

We denote these weight factors by w_i , such that the $SO(4)$ representation labeled by i couples to the global Higgs with Yukawa coupling

$$\xi_{U,i} = w_i \xi_U, \quad \xi_{D,i} = w_i \xi_D, \quad \xi_{E,i} = w_i \xi_E. \quad (4.6)$$

The various possible $SO(5)$ and $SO(4)$ symmetric Yukawa couplings for the above representations and the respective factors w_i are summarized in Tables 2 and 3 (see App. B for further details). We see, in particular, that the number of fermion states that couple to the global Higgs depends very much on the assumed representation of both the scalar and the fermions.

We will assume all masses and couplings in the fermionic Lagrangian to be real for definiteness.¹⁰ Notice that we can write two independent Yukawas of the type $\Phi \bar{Q} U$ and $\Phi \bar{Q} \gamma^5 U$. We find it more convenient to switch to the two operators $\Phi \bar{Q} P_R U$ and $\Phi \bar{Q} P_L U$, whose coefficients we will generally denote by ξ and ξ' respectively.

¹⁰In realistic scenarios the phases are constrained by CP violation. Constructing a fully realistic flavor sector is not the goal of this work.

proto-Yukawa	$\bar{F}\Phi S'$	$\bar{F}A'\Phi$	$\bar{F}B'\Phi$	$\bar{F}\Psi F'$	$\bar{S}\text{tr}\Psi B'$	$\text{tr}\bar{A}\Psi A'$	$\text{tr}\bar{B}\Psi B'$	$\text{tr}\bar{B}\Psi A'$
$\phi \bar{s}s'$	1	—	$\frac{2}{\sqrt{5}}$	$\frac{2}{\sqrt{5}}$	1	—	$\frac{3}{2\sqrt{5}}$	—
$\phi \bar{f}f'$	—	$\frac{1}{\sqrt{2}}$	$\frac{1}{\sqrt{2}}$	$\frac{1}{2\sqrt{5}}$	—	$\frac{3}{4\sqrt{5}}$	$\frac{3}{4\sqrt{5}}$	$\frac{\sqrt{5}}{4}$
$\phi \bar{a}a'$	—	—	—	—	—	$\frac{1}{2\sqrt{5}}$	—	—
$\phi \bar{b}b'$	—	—	—	—	—	—	$\frac{1}{2\sqrt{5}}$	—

Table 2. The $SO(4)$ multiplets that couple to the global Higgs, for various choices of the dimension-4 proto-Yukawa interactions (as specified in the first row). The entries give the weight factors w_i as defined in Eq.(4.6). We use the notation $S \leftrightarrow \mathbf{1}$, $F \leftrightarrow \mathbf{5}$, $A \leftrightarrow \mathbf{10}$ and $B \leftrightarrow \mathbf{14}$ to indicate the various fermionic $SO(5)$ representations considered, as well as $s \leftrightarrow \mathbf{1}$, $f \leftrightarrow \mathbf{4}$, $a \leftrightarrow \mathbf{6}$ and $b \leftrightarrow \mathbf{9}$ for the $SO(4)$ representations. Φ is understood as a fiveplet of $SO(5)$, while the matrix Ψ is to be interpreted as the $\mathbf{14}$ representation of $SO(5)$.

proto-Yukawa	$\bar{F}\Phi\Phi^\dagger F'$	$\bar{S}\Phi^\dagger B'\Phi$	$\Phi^\dagger \bar{A}A'\Phi$	$\Phi^\dagger \bar{B}B'\Phi$	$\Phi^\dagger \bar{B}A'\Phi$
$\phi \bar{s}s'$	2	$\frac{4}{\sqrt{5}}$	—	$\frac{8}{5}$	—
$\phi \bar{f}f'$	—	—	1	1	1

Table 3. Same as Table 2, but for the dimension-5 proto-Yukawa interactions.

For the lighter up-type quarks one can mimic the construction described in more detail for the top quark sector in Subsection 4.1, which falls in the “ $\bar{F}\Phi S$ ” category of Table 2. Alternatively, one can use the less minimal variant that replaces the $\mathbf{1}_{\frac{2}{3}}$ with the $\mathbf{14}_{\frac{2}{3}}$ of $SO(5) \times U(1)_X$, corresponding to the “ $\bar{F}B\Phi$ ” category. For the bottom sector (specifically the b_R) one can see from Table 1 that the candidate representations are the $\mathbf{5}_{-\frac{1}{3}}$ and the $\mathbf{10}_{\frac{2}{3}}$. The first case requires the introduction of an additional composite $\mathbf{5}_{-\frac{1}{3}}$ partner of the (t_L, b_L) doublet, in order to be able to write down the $\bar{F}\Psi F$ category of Table 2 for the bottom sector. This would be in addition to the composite $\mathbf{5}_{\frac{2}{3}}$ associated with the top sector, which is also a composite partner of the (t_L, b_L) doublet. Thus, the choice of a composite $\mathbf{5}_{-\frac{1}{3}}$ that partners with b_R leads to a rather non-minimal scenario. If one insists on dim-4 proto-Yukawa interactions, such that Ψ , which hosts the global Higgs, would transform in the $\mathbf{14}$ of $SO(5)$, one increases even more the level of complexity. The second option is more minimal in comparison: with the b_R composite partner transforming in the $\mathbf{10}_{\frac{2}{3}}$ of $SO(5) \times U(1)_X$ one can write a dim-4 proto-Yukawa interaction using the global Higgs arising from a $\mathbf{5}$ (denoted by Φ before), and without enlarging the top sector. We will therefore take this second case, replicated for all the down-type quarks as a reference example.

4.3 Benchmark Models

We now define a set of benchmark scenarios in order to illustrate the typical embeddings of the global Higgs in composite Higgs models. In a forthcoming publication, a collider analysis will be carried out for these scenarios [21].

Quark Benchmarks:

- MCHM_{5,1,10}: $(Q_i, U_i, D_i) = (\mathbf{5}_{\frac{2}{3}}, \mathbf{1}_{\frac{2}{3}}, \mathbf{10}_{\frac{2}{3}})$, $\phi \subset \mathbf{5}_0$,
- MCHM_{5,14,10}: $(Q_i, U_i, D_i) = (\mathbf{5}_{\frac{2}{3}}, \mathbf{14}_{\frac{2}{3}}, \mathbf{10}_{\frac{2}{3}})$, $\phi \subset \mathbf{5}_0$,
- MCHM_{14,14,10}: $(Q_i, U_i, D_i) = (\mathbf{14}_{\frac{2}{3}}, \mathbf{14}_{\frac{2}{3}}, \mathbf{10}_{\frac{2}{3}})$, $\phi \subset \mathbf{14}_0$.

The first two models require the global Higgs to be embedded in the $\mathbf{5}$ representation, while for the third one we chose the $\mathbf{14}$. The last model uses the “ $\text{tr } \bar{B}\Psi B$ ” proto-Yukawa structure for the up sector, and the “ $\text{tr } \bar{B}\Psi A$ ” proto-Yukawa structure for the down sector, following the notation of Table 2. These three benchmark models are understood to be characterized by order one proto-Yukawa couplings (we will be more precise in Sec. 6) and hierarchical mixing angles (see the discussion after Eqs. (2.1) and (2.2) in Section 2).

As already mentioned in Section 2 we will also consider the scenario with hierarchical Yukawas and order one mixing angles, as a “most minimal” example where the global Higgs properties are only sensitive to the top sector:

- MCHM_{5,1}: $(Q_3, U_3) = (\mathbf{5}_{\frac{2}{3}}, \mathbf{1}_{\frac{2}{3}})$. The representations of the composite partners for the SM fermions other than $q_L = (t_L, b_L)$ and t_R need not be specified in this case since they play a negligible role. The global Higgs is in a $\mathbf{5}_0$.

Lepton Benchmarks:

The lepton sector can potentially play a role in the coupling of the global Higgs to two photons, and as for the case of quarks vis-à-vis the two-gluons amplitude, they can introduce additional model-dependence. We therefore fix two benchmark scenarios in the leptonic sector, that apply for each of the four quark sector scenarios defined above:

- A leptonic anarchic scenario with $(L_i, E_i) = (\mathbf{5}_{-1}, \mathbf{1}_{-1})$, which falls in the “ $\bar{F}\Phi S$ ” category of Table 2.
- A non-anarchic scenario analogous to the MCHM_{5,1} above, where all the composite lepton proto-Yukawa couplings are small, and therefore the heavy leptonic states have a minimal impact on the phenomenology of the global Higgs. In this case, the representations of the composite partners of the SM leptons need not be specified.

As we will see, this will illustrate that the impact of the leptonic sector can be relatively minor. Notice also that here we will remain agnostic about the composite states related to the neutrino sector, and assume, conservatively, that they do not contribute.

5 Effective One-loop Couplings to the SM Gauge Bosons

As mentioned before, the global Higgs couplings to massless gauge bosons such as the gluon and the photon as well as the couplings to the transverse polarizations of the electroweak gauge bosons are induced by one-loop processes which are sensitive to the details of the particles running in the loop. These couplings are very important for phenomenological studies and in this section we estimate them in the different benchmark models defined in the previous section.

The effective one-loop coupling of the global Higgs to a gluon pair proceeds in complete analogy to the SM calculation. The result can be encoded into the dimension-5 effective term

$$\mathcal{L}_{\phi gg}^{\text{eff}} = -\frac{\alpha_s N_{\phi gg}}{12\pi\hat{f}} \phi G_{\mu\nu}^a G_a^{\mu\nu} , \quad (5.1)$$

where

$$N_{\phi gg} = \frac{3}{4}\hat{f} \sum_i \frac{M'_i}{M_i} A_{1/2} \left(\frac{m_\phi^2}{4M_i^2} \right) , \quad (5.2)$$

and the sum runs over all the quark states of mass M_i that couple to the global Higgs ϕ with Yukawa strength $M'_i = \partial_\phi M_i(\phi)|_{\phi=0}$.¹¹ The $A_{1/2}(\tau)$ is the standard loop function, which is given in Appendix C. It saturates to 4/3 in the limit that the fermion is heavy compared to m_ϕ , and vanishes in the opposite limit.

The coupling of the global Higgs to the EW gauge bosons is similarly given by

$$-\frac{\alpha}{s_W^2} \frac{N_{\phi WW}}{8\pi\hat{f}} \phi W_{\mu\nu}^i W^{\mu\nu i} - \frac{\alpha}{c_W^2} \frac{N_{\phi BB}}{8\pi\hat{f}} \phi B_{\mu\nu} B^{\mu\nu} , \quad (5.3)$$

where we can write $N_{\phi WW} = N_{\phi\gamma\gamma} - N_{\phi BB}$ with

$$N_{\phi\gamma\gamma} = \frac{m_a^2 - m_\rho^2}{m_a^2} A_1 \left(\frac{m_\phi^2}{4m_a^2} \right) + \hat{f} \sum_i \frac{M'_i}{M_i} N_c Q_i^2 A_{1/2} \left(\frac{m_\phi^2}{4M_i^2} \right) , \quad (5.4)$$

$$N_{\phi BB} = \hat{f} \sum_i \frac{M'_i}{M_i} N_c Y_i^2 A_{1/2} \left(\frac{m_\phi^2}{4M_i^2} \right) , \quad (5.5)$$

and $N_c = 3$ (1) is the number of colors for quarks (leptons). One then gets the couplings to $\gamma\gamma$, ZZ , γZ and W^+W^- :

$$-\frac{\alpha}{8\pi\hat{f}} \left(N_{\phi\gamma\gamma} \phi F_{\mu\nu} F^{\mu\nu} + \frac{N_{\phi ZZ}}{s_W^2 c_W^2} \phi Z_{\mu\nu} Z^{\mu\nu} + \frac{2N_{\phi Z\gamma}}{s_W c_W} \phi F_{\mu\nu} Z^{\mu\nu} + \frac{2N_{\phi WW}}{s_W^2} \phi W_{\mu\nu}^+ W^{-\mu\nu} \right) , \quad (5.6)$$

where

$$N_{\phi ZZ} = c_W^4 N_{\phi WW} + s_W^4 N_{\phi BB} , \quad N_{\phi\gamma Z} = N_{\phi WW} - s_W^2 N_{\phi\gamma\gamma} . \quad (5.7)$$

¹¹For simplicity, and because it is a good approximation, we will neglect EWSB effects.

The first term in Eq. (5.4) corresponds to the charged pair of $SO(5)/SO(4)$ gauge bosons that receive a contribution $\sqrt{m_a^2 - m_\rho^2}$ to their mass from the breaking at \hat{f} . The well-known loop function $A_1(\tau)$ (see Appendix C) reaches the asymptotic value -7 when the spin-1 resonance is much heavier than the global Higgs. Notice that the spin-1 contribution is completely parallel to the one from the charged W 's in the SM Higgs case, with the pair of heavy charged vector fields playing the role of the SM W^\pm . Here, however, we expect to be much closer to the saturation limit of the loop function, since the spin-1 resonances are taken to be heavy (see the discussion in Section 2). The second term in Eq. (5.4), as well as Eq. (5.5), includes the contribution from all the fermions that couple to the global Higgs, including quark and lepton fields.

In order to estimate the multiplicity factors $N_{\phi XX}$ with $X = g, \gamma, B$ for each of the benchmark scenarios defined in the previous subsection, we assume that the fermions have a common vector-like mass, $M_Q = M_U = M_D = M_\psi$. If the vectorlike mass dominates over the global symmetry breaking effects, and assuming also small mixing with the elementary sector, the fermions are approximately degenerate in mass with $M_i \sim M_\psi$.¹² We can then factor out a common loop function $A_{\frac{1}{2}}(m_\phi^2/4M_\psi^2)$ and compute the sum as¹³

$$\sum_i \frac{M'_i}{M_i} = \frac{d(\det \mathcal{M})/d\hat{f}}{\det \mathcal{M}} \approx -2 \frac{\hat{f}}{M_\psi^2} (\bar{N}_{\phi gg}^U \text{tr} \xi'_U \xi_U^T + \bar{N}_{\phi gg}^D \text{tr} \xi'_D \xi_D^T) , \quad (5.8)$$

where the remaining traces are over the 3 generations, and the $\bar{N}_{\phi gg}^{U,D}$ are the sums over the $SO(4)$ multiplicities N_i , weighted by the factors w_i^2 , where the w_i are given in Table 2. The $\bar{N}_{\phi gg}^{U,D}$ are summarized in Table 4. Analogously, we can obtain

$$\sum_i \frac{M'_i}{M_i} N_c Q_i^2 \approx -2 \frac{\hat{f}}{M_\psi^2} (3 \bar{N}_{\phi \gamma \gamma}^U \text{tr} \xi'_U \xi_U^T + 3 \bar{N}_{\phi \gamma \gamma}^D \text{tr} \xi'_D \xi_D^T + \bar{N}_{\phi \gamma \gamma}^E \text{tr} \xi'_E \xi_E^T) , \quad (5.9)$$

where $\bar{N}_{\phi \gamma \gamma}^{U,D,E}$ are the sums over the $SO(4)$ multiplicities, weighted by the charges Q_i^2 and the factors w_i^2 as before. The factors $\bar{N}_{\phi BB}^{U,D,E}$ for the hypercharge are defined analogously. The charges and hypercharges can be read off from Table 1 for each benchmark model. It should be noted that the tensor couplings of the electroweak gauge bosons are expected to compete with the longitudinal couplings (arising from the operator \mathcal{O}_H at tree level) only for large Yukawa couplings and multiplicities. Moreover, we point out that the tree and

¹²As we will detail in the accompanying work [21], our analytic expressions for the loop processes can be quite effectively used even when these assumptions are not fulfilled, by using Eq. (5.8) to *define* an effective mass scale M_ψ (provided it does not vanish; see next footnote). The $\phi\gamma\gamma$ and ϕBB processes can similarly be used to define effective scales via Eq. (5.9) and the analogous equation with hypercharge weighting. However, in the bulk of the parameter space of each model, the three scales are quite similar and, therefore, to a good approximation, one can reduce the model dependence to a single parameter, that one can characterize as “the scale of spin-1/2 resonances”.

¹³Note that for this result to be non-vanishing both ξ and ξ' must be non-zero. We recall that in the presence of the “wrong-chirality” structure with coefficient ξ' , the SM Higgs potential may acquire a log sensitivity to the compositeness scale Λ . This mild dependence is not necessarily a problem. If one has a situation with a vanishing ξ' , the sum in Eq. (5.8) is proportional to the elementary-composite mixing, which we have ignored in the derivation.

Benchmark	$\bar{N}_{\phi gg}^U$	$\bar{N}_{\phi gg}^D$	$\bar{N}_{\phi\gamma\gamma}^U$	$\bar{N}_{\phi\gamma\gamma}^D$	$\bar{N}_{\phi\gamma\gamma}^E$	$\bar{N}_{\phi BB}^U$	$\bar{N}_{\phi BB}^D$	$\bar{N}_{\phi BB}^E$
MCHM _{5,1,10}	1	2	$\frac{4}{9}$	$\frac{17}{9}$	1	$\frac{4}{9}$	$\frac{25}{18}$	1
MCHM _{5,14,10}	$\frac{14}{5}$	2	$\frac{101}{45}$	$\frac{17}{9}$	1	$\frac{157}{90}$	$\frac{25}{18}$	1
MCHM _{14,14,10}	$\frac{27}{20}$	$\frac{5}{4}$	$\frac{57}{40}$	$\frac{85}{72}$	1	$\frac{81}{80}$	$\frac{125}{144}$	1
MCHM _{5,1}	1	—	$\frac{4}{9}$	—	—	$\frac{4}{9}$	—	—

Table 4. Fermionic multiplicity factors entering the effective couplings of the global Higgs to two gluons or two EW gauge bosons, given in Eqs (5.8) and (5.9).

loop level couplings have a different scaling with \hat{f} or equivalently, for fixed Global Higgs mass, with the quartic coupling λ . The typical size of the Yukawa and quartic interactions will be estimated in the next section.

One may wonder if higher order (finite effects) could give large corrections to the 1-loop results, given the large multiplicities involved. One can see, however, that the higher order corrections involving additional heavy fermion loops enter only at 3-loop order and would not be expected to give a large effect. Rather, we expect the higher-order corrections to be dominated by QCD, very much as in the SM. While a more precise treatment would include the QCD K -factors, to be on the conservative side, we will not include any such corrections. One should, however, keep in mind that they will give an additional enhancement to the rates involving two gluons or two photons.

6 Running Couplings in the Composite Sector

In the presence of large $SO(5)$ matter representations such as **10** and **14** (in particular when repeated for all 3 generations) the RG running of the Yukawa couplings and of the global Higgs quartic coupling λ from the compositeness scale Λ down to the global Higgs mass scale m_ϕ has to be taken into account. We will see below that the beta function of the Yukawa couplings is always positive because of loops of the global Higgs. This implies that the Yukawa couplings develop a Landau pole at relatively low energies, and thus that the strong dynamics develops at a scale Λ not far above the global Higgs mass. We shall identify this strong coupling scale with the compositeness scale. Below the strong coupling scale, couplings are expected to quickly decrease, so that the composite states can be described as well-defined propagating states.¹⁴

¹⁴ We must notice that the masses of vector resonances may in principle be higher than Λ , which means they cannot be described consistently by the theory. However, the imprint of these resonances on the global Higgs properties is only characterized by $r_v = f/\hat{f}$, and thus does not depend on the resonance masses. The kinetic terms of the vector resonances can be consistently sent to zero by taking $g_\rho \rightarrow \infty$. In this limit the linear sigma model with gauge fields is strictly equivalent to a non-linear sigma model [20], in which no physical particle is present above Λ .

Benchmark	ξ^2/ξ_{eff}^2	$\xi(\mu = m_\phi)$	ϵ	λ_{min}	λ_{max}	$\lambda/\xi^2 _{\text{fix}}$
MCHM _{5,1,10}	$\frac{1}{216}$	0.6 (0.5)	$\frac{1}{162}$	0.24	2.6	1.17
MCHM _{5,14,10}	$\frac{5}{1728}$	0.5 (0.4)	$\frac{11}{3456}$	0.12	2.5	1.02
MCHM _{14,14,10}	$\frac{5}{936}$	0.6 (0.5)	—	—	—	—
MCHM _{5,1}	$\frac{1}{24}$	1.6 (1.2)	$\frac{1}{12}$	2.3	3.9	1.11

Table 5. Yukawa couplings and scalar self-couplings in our various benchmark scenarios. See text for details.

We work at leading order in large multiplicities, and at 1-loop order. It turns out that the running of the Yukawa couplings is dominated by the wave-function renormalization of the global Higgs, and hence can be expressed in terms of ¹⁵

$$\xi_{\text{eff}}^2 = 4N_c \left(N^U [\text{tr } \xi_U \xi_U^T + \text{tr } \xi'_U \xi'^T_U] + N^D [\text{tr } \xi_D \xi_D^T + \text{tr } \xi'_D \xi'^T_D] \right), \quad (6.1)$$

where N^U and N^D are the multiplicities of the $SO(4)$ representations, weighted by the group-theoretical factors, and hence they coincide with the quantities encountered in the loop expressions for the ϕgg coupling

$$N^U = \bar{N}_{\phi gg}^U, \quad N^D = \bar{N}_{\phi gg}^D, \quad (6.2)$$

which for our various scenarios were given in Table 4. The RG equation for ξ_{eff} reads

$$\mu \frac{d\xi_{\text{eff}}^2}{d\mu} \approx \frac{\xi_{\text{eff}}^4}{16\pi^2}, \quad (6.3)$$

The term above arises from the global Higgs wavefunction renormalization, when neglecting subdominant (*i.e.* not enhanced by multiplicities) terms coming from vertex and fermion wavefunction renormalization.¹⁶ Similarly, we have neglected the effects of gauge couplings which would also induce a differential running between the different ξ_i . It is also worth noting that, at 1-loop order, λ does not enter into the RG equation for ξ_{eff} .

We now assume that ξ_{eff} reaches a value of order 4π at the compositeness scale $\Lambda \approx 3m_\phi$. This hierarchy is somewhat arbitrarily chosen to indicate a gap between m_ϕ and Λ without taking it so large that an extreme tuning would be involved. With this boundary condition, we find that at the scale m_ϕ , the coupling ξ_{eff} is

$$\xi_{\text{eff}}(m_\phi) \approx 8.7. \quad (6.4)$$

¹⁵We include here only the quark states (which overwhelm the contribution from the lepton states).

¹⁶We have checked that accounting for such subleading effects the resulting corrections are indeed negligible for our purposes of estimating the Yukawa couplings at the scale m_ϕ . The only exception is the minimal model MCHM_{5,1}, for which we have included the subleading terms to obtain our numbers (but still neglecting the lepton sector).

To continue further, we make the additional assumption that all the relevant Yukawa couplings are similar. Setting them equal ($\xi = \xi_{U,D} = \xi'_{U,D}$) we find at the scale m_ϕ the values reported in the third column of Table 5. The number in parenthesis corresponds to taking $\Lambda \approx 10m_\phi$, and is included only for comparison. Under our simplifying assumptions, these are the relevant couplings when computing finite effects, such as the loop induced couplings which are dominated by momenta of order m_ϕ .¹⁷

We now turn to the quartic interaction of the global Higgs. In order to estimate values for λ at $\mu = m_\phi$, we consider its 1-loop RGE, assuming our estimates for ξ in Table 5. The 1-loop RG equation of the quartic is given by¹⁸

$$\mu \frac{d\lambda}{d\mu} \approx \frac{1}{16\pi^2} (26\lambda^2 + 2\lambda\xi_{\text{eff}}^2 - \epsilon\xi_{\text{eff}}^4), \quad (6.5)$$

where the value of ϵ is suppressed by the multiplicities and is reported in Table 5. We can see there are actually two distinct possibilities: if λ is sufficiently small, it is driven to a negative value at Λ as a result of the renormalization by the Yukawa interactions. Above a certain threshold, it is driven instead to a Landau pole at Λ . This is similar to the well-known situation for the Higgs quartic coupling in the SM. These two limit cases can be taken to define an upper and a lower bound for the value of λ at $\mu = m_\phi$. Below we denote these extreme values by λ_{min} and λ_{max} .

We find that for $\Lambda = 3m_\phi$, the quartic coupling is driven negative when $\lambda \approx 0.24$ at $\mu = m_\phi$ in the MCHM_{5,1,10}. For the MCHM_{5,1} this value is 2.3. It is larger because multiplicities are smaller in this scenario. On the opposite end, the maximum value of the quartic at $\mu = \Lambda$ is given by naive dimensional analysis and is $\lambda = (4\pi)^2/3!$, where $\xi_{\text{eff}} \equiv \sqrt{N}\xi \sim 4\pi$ and $N \equiv \sum_i 4N_c N_i$.¹⁹ From these values at the strong coupling scale one obtains $\lambda(\mu = m_\phi) = \lambda_{\text{max}} \approx 2.6$ for the MCHM_{5,1,10}. For the MCHM_{5,1}, taking into account subleading corrections, one has that $\lambda(\mu = m_\phi) = \lambda_{\text{max}} \approx 3.9$. Thus, the values of λ are in an even narrower range in that case. The ranges for λ are summarized in Table 5.

In connection to this, we point out that the ratio λ/ξ^2 displays a (quasi) IR fixed point which is also shown in Table 5, as discussed in [4].²⁰ While for the MCHM_{5,1} the IR fixed point is approached sufficiently fast, for the other models the running over three e-folds is not sufficient to come close to the fixed point. As a result, we must accept an intrinsic degree of uncertainty in the coupling λ at $\mu = m_\phi$ in the large multiplicity models, due to the underlying strong dynamics. Based on the above considerations we will allow λ to take values in the range $[\xi^2, \lambda_{\text{max}}]$, where ξ^2 (which is somewhat above λ_{min}) and λ_{max} can be read from Table 5.²¹ In most of this range, λ is driven to its strong coupling (NDA) value near $\Lambda = 3m_\phi$. Only in the vicinity of the lower limit can λ stay perturbative when $\mu \sim \Lambda$.

¹⁷We note that reproducing the top quark mass may require taking a slightly larger ξ_t . Since other couplings may be slightly smaller, we regard our numerical estimates as representing an average that characterizes the overall combined effect of the multiplicity of states.

¹⁸For MCHM_{14,14,10}, we would have to consider the simultaneous running of two quartic couplings (see App. A).

¹⁹The $3!$ is the combinatorial factor that we did not factor out in our definition of the quartic coupling in Eq. (3.3).

²⁰These fixed point values can decrease somewhat after including the effects of the gauge interactions.

²¹Comparing the MCHM_{5,1,10} and MCHM_{5,14,10} the slightly different lower limits in the range for λ are

Notice also that the quartic coupling at $\mu = m_\phi$ is always well below its strong coupling value, as estimated by NDA.

These estimates of the couplings in the composite sector at the global Higgs mass scale allows for more precise predictions of the global Higgs properties. In particular, they allow one to estimate the one-loop effective couplings in a given scenario, and to tie the global Higgs mass to the $SO(5)$ breaking scale \hat{f} .

7 Decays

The decay width of the global Higgs into SM fermions is universally given by

$$\Gamma_{\phi \rightarrow f \bar{f}} = N_c \frac{m_f^2}{8\pi \hat{f}^2} m_\phi, \quad (7.1)$$

and is dominated by the top quark. The partial widths into Goldstone bosons are given by

$$\Gamma_{\phi \rightarrow hh} = \Gamma_{\phi \rightarrow Z_L Z_L} = \frac{1}{2} \Gamma_{\phi \rightarrow W_L^+ W_L^-} = \frac{r_v^2}{32\pi} \frac{m_\phi^3}{\hat{f}^2}, \quad (7.2)$$

where we neglect EWSB effects. These are the dominant decay modes.

The one-loop decays into SM gauge bosons via loops of vector-like fermions and $SO(5)/SO(4)$ composite vector bosons are given by

$$\Gamma_{\phi \rightarrow gg} = \alpha_s^2 \frac{N_{\phi gg}^2}{72\pi^3} \frac{m_\phi^3}{\hat{f}^2}, \quad (7.3)$$

$$\Gamma_{\phi \rightarrow \gamma\gamma} = \alpha^2 \frac{N_{\phi\gamma\gamma}^2}{256\pi^3} \frac{m_\phi^3}{\hat{f}^2}, \quad \Gamma_{\phi \rightarrow Z_T Z_T} = \frac{\alpha^2}{s_W^4 c_W^4} \frac{N_{\phi ZZ}^2}{256\pi^3} \frac{m_\phi^3}{\hat{f}^2}, \quad (7.4)$$

$$\Gamma_{\phi \rightarrow \gamma Z_T} = \frac{\alpha^2}{s_W^2 c_W^2} \frac{N_{\gamma Z}^2}{128\pi^3} \frac{m_\phi^3}{\hat{f}^2}, \quad \Gamma_{\phi \rightarrow W_T^+ W_T^-} = \frac{\alpha^2}{s_W^4} \frac{N_{\phi WW}^2}{128\pi^3} \frac{m_\phi^3}{\hat{f}^2}. \quad (7.5)$$

The total width for loop-induced decays into transverse electroweak bosons can be written as

$$\Gamma_{\phi \rightarrow V_T V_T'} = \alpha^2 \frac{3s_W^{-4} N_{\phi WW}^2 + c_W^{-4} N_{\phi BB}^2}{256\pi^3} \frac{m_\phi^3}{\hat{f}^2}. \quad (7.6)$$

Mixed decays into one SM fermion and one of its partners may also be possible. The most important channels are typically the ones involving the right handed top, and to a lesser extend the left handed top-bottom doublet, provided the corresponding partners are not too heavy. Denoting the mixing angles by s_R and s_L respectively, one finds ²²

$$\Gamma_{\phi \rightarrow t' \bar{t}, t \bar{t}'} = N_c \frac{|\xi_{U,1}|^2 s_R^2}{4\pi} m_\phi \gamma_\psi^2, \quad \Gamma_{\phi \rightarrow q' \bar{q}, q \bar{q}'} = N_c \frac{|\xi_{U,4}|^2 s_L^2}{4\pi} m_\phi \gamma_\psi^2, \quad (7.7)$$

roughly consistent with the slightly different fixed point values. For the MCHM_{5,1}, on the other hand, the uncertainty in λ is narrower than the assumed range, since the IR fixed point is approached more quickly.

²² Note that the mixed Yukawa interaction is $\mathcal{L} = -s_R \xi_{U,1} \phi \bar{Q}_L t_R + \text{h.c.}$ The vectorlike masses split into $c_R M_\psi$ (the U state) and M_ψ (the Q state). For large mixing, Q and U are approximate mass eigenstates, and the decay proceeds to t and $t' = Q$. If the mixing is smaller, the mass eigenstates become approximately degenerate again and are roughly equal mixtures of Q and U . The interaction is thus between $Q_L = (t' + t'')/\sqrt{2}$ and t_R , and the decay proceeds to two states t' and t'' . The net effect is the same.

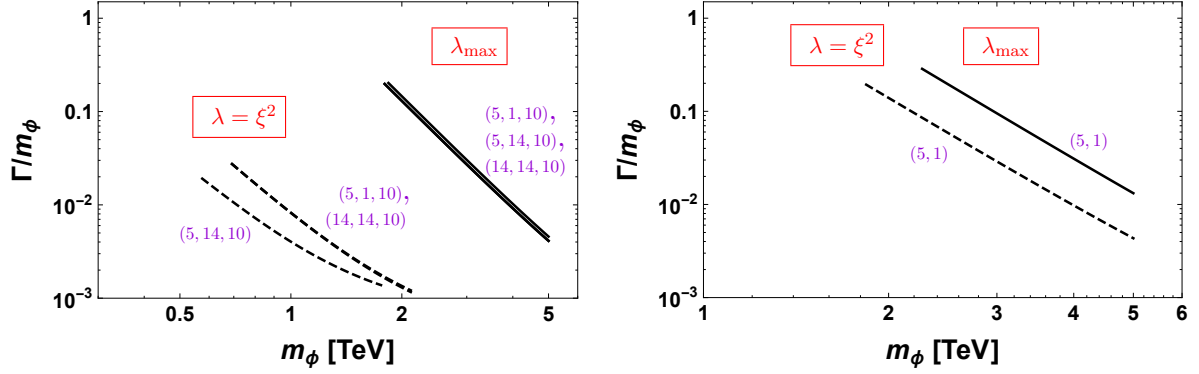


Figure 1. Total width of the global Higgs in the case that the decays to fermion resonances are forbidden. The plot shows curves for $\lambda = \xi^2$ (dashed lines) and $\lambda = \lambda_{\max}$ (continuous lines), as given in Table 5 for the different models. The minimum m_ϕ is determined by $\hat{f} \geq f$.

where we have neglected EWSB effects (in particular we neglect the top and bottom squared masses against those of t' , q' and ϕ), and we have defined $\gamma_\psi = 1 - \frac{M_\psi^2}{m_\phi^2}$. The subindices 1 and 4 on ξ_U indicate the $SO(4)$ representation of the top partners. They are related to the $SO(5)$ symmetric Yukawa ξ_U via the factors w_i in Table 2 and 3.

If the fermion resonances are sufficiently light, it is possible for the global Higgs to decay into a heavy fermion pair. We will give the corresponding partial widths in a simplified limit in Subsection 7.2.

7.1 Case I: Closed Decay Channels into Fermion Resonances

We assume first that the decays of the global Higgs into SM fermion partners are kinematically forbidden, e.g. $M_i > m_\phi$. This assumption also has implications for the loop decays, which are controlled by the relative contribution to the fermion masses from global symmetry breaking versus symmetry preserving effects, as described in Sec. 5. This relative importance is characterized by $(\xi \hat{f})^2 / M_\psi^2 = (\xi^2 / 2\lambda)(m_\phi / M_\psi)^2 \lesssim \xi^2 / 2\lambda$, which can be seen to be at most of order one in the lower end of the range for λ (see Table 5), hence the approximate formulas Eqs. (5.8), (5.9) are valid. In most of the considered range for λ , the $(\xi \hat{f})^2 / M_\psi^2$ factor will in fact induce an important suppression for such decays, in addition to the 1-loop suppression. For illustration, we will use $M_\psi = m_\phi$ in Eqs. (5.8) and (5.9), and take the value $A_{1/2}(1/4) \approx 1.42$ for the fermion loop function (slightly above the asymptotic value of $4/3$).

We then have a rather predictive case, since the dominant features depend on only three parameters, that can be taken as the global Higgs mass m_ϕ , the quartic coupling λ , and the Higgs decay constant f . The latter controls the deviations of the pNGB Higgs properties from the SM limit, and can be constrained by Higgs measurements, which as illustrated in [12], can be fairly model-dependent. For concreteness, we will take $f = 800$ GeV, which should allow to satisfy comfortably the current Higgs constraints for a wide choice of parameters in the fermionic sector. In addition, such a choice also allows for generic consistency with EW precision measurements (see, for example, [22]). A more detailed study of Higgs and EW precision constraints is beyond the scope of this work, and is not

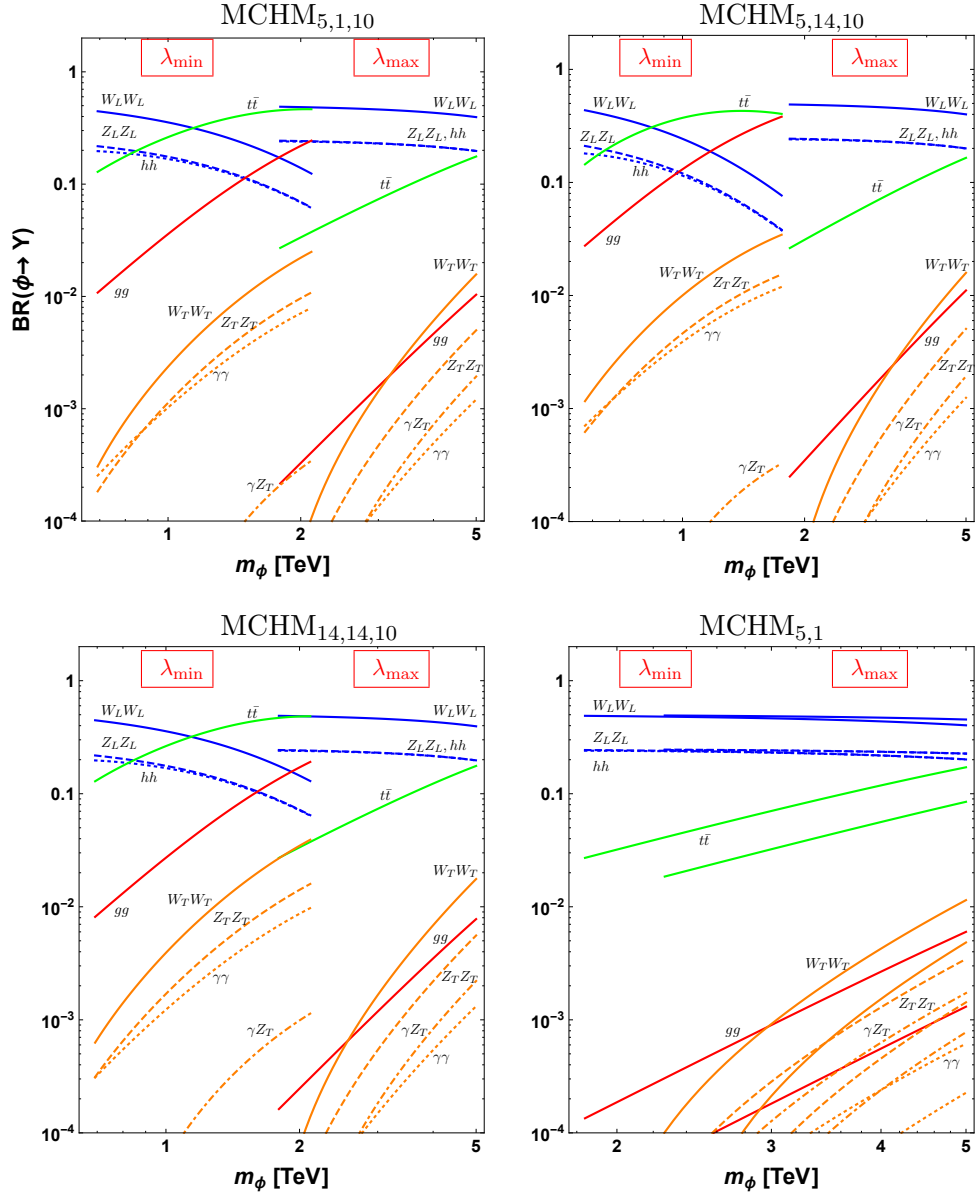


Figure 2. Branching fractions of the global Higgs in the $\text{MCHM}_{5,1,10}$, $\text{MCHM}_{5,14,10}$, $\text{MCHM}_{14,14,10}$, $\text{MCHM}_{5,1}$ scenarios, assuming that decays into fermion resonances are forbidden. Both extreme values $\lambda = \{\xi^2, \lambda_{\max}\}$ of the global Higgs quartic coupling are shown, and we fix $f = 800$ GeV and $M_\psi = m_\phi$. Blue lines correspond to $W_L W_L$ (solid), $Z_L Z_L$ (dashed), hh (dotted) final states. The green line is $t\bar{t}$. The red line is gg and orange lines correspond to $W_T W_T$ (solid), $Z_T Z_T$ (dashed), $\gamma\gamma$ (dotted), γZ_T (dash-dotted). The minimum m_ϕ is determined by $\hat{f} \geq f$.

expected to change our conclusions. Thus, fixing f allows us to focus on the properties of the global Higgs, as controlled by the two remaining parameters, m_ϕ and λ , which barely affect the SM Higgs phenomenology.²³ Note that Eqs. (3.4) and (3.11) imply that $m_\phi \geq \sqrt{2\lambda}f$, so that for a given value of λ one obtains a minimum global Higgs mass. One

²³ The low-energy effects of the global Higgs are described by loop-generated dimension-6 operators and tree-level dimension-8 operators.

could also be worried about potential direct lower limits on m_ϕ . Adapting the ATLAS heavy Higgs search of Ref. [23], we obtain that the global Higgs must be roughly heavier than about 750 GeV [21].

An interesting feature of the global Higgs couplings to transverse electroweak gauge bosons is that they are dominated by the loops of the spin-1 (coset) resonances for large values of λ . In this case these couplings are mainly controlled by the r_v parameter (the spin-1 amplitude scales as $1 - r_v$, as can be seen from Eq. (5.4)), up to small corrections from the fermion loops, and thus depend only mildly on the fermion sector. On the other hand the EW couplings at small λ , as well as the gluon coupling, are fully dependent on the sector of fermion resonances.

The total width of the global Higgs is dominated by the decays into the $SO(5)/SO(4)$ Goldstone bosons and into pairs of top quarks. These contributions do not depend on the details of the fermion sector, so that one has in general

$$\frac{\Gamma_{\text{tot}}}{m_\phi} \approx \frac{r_v^2}{32\pi} \frac{m_\phi^2}{\hat{f}^2} + \frac{3m_t^2}{8\pi\hat{f}^2}, \quad (7.8)$$

to a very good approximation. The total widths are shown in Fig. 1. We use the relation $m_\phi^2/\hat{f}^2 = 2\lambda$, together with the estimates of λ derived in Sec. 6. It turns out that the total width ranges from $\Gamma_\phi/m_\phi = \mathcal{O}(10^{-3})$ to $\mathcal{O}(0.1)$. The global Higgs is thus always narrow enough so that the “narrow width approximation” applies.

We also show in Fig. 2 the branching fractions for our benchmark scenarios, displayed as a function of m_ϕ . We do this for the two extreme estimates of the global Higgs quartic coupling $\lambda = \xi^2$ and $\lambda = \lambda_{\text{max}}$, as determined in Sec. 6. We observe that $\Gamma_{\phi \rightarrow \gamma\gamma}$ is smaller than $\Gamma_{\phi \rightarrow W^+W^-}$ and $\Gamma_{\phi \rightarrow ZZ}$ by several orders of magnitude at $m_\phi = 750$ GeV. Due to the LHC13 bounds on the diboson ZZ , WW channels from ATLAS [24] and CMS [25], the possibility of interpreting the 750 GeV diphoton excess [26, 27] as originating from the resonant production of a narrow global Higgs with $m_\phi = 750$ GeV is excluded. It turns out that the branching fractions into two gluons, two photons, and into the transverse components of the weak gauge bosons become more important for a heavier global Higgs (see Fig. 2). Such enhancement of the couplings to transverse gauge bosons is potentially interesting for production of the global Higgs at the LHC and will be explored in more detail in the accompanying Ref. [21].

7.2 Case II: Open Decay Channels into Fermion Resonances

Clearly, when decays into fermionic resonances (or mixed decays into a SM fermion and one of its partners) are kinematically open, the branching fractions are sensitive to the details of the new fermionic sector. For illustration, we consider the case where all the fermion resonances are light compared to the global Higgs. In this case, all possible two-body decay channels are open. Neglecting the small M_ψ^2/m_ϕ^2 terms, *i.e.* taking all $\gamma_\psi = 1$ in Eq. (7.7), and assuming universal $SO(5)$ proto-Yukawa couplings $\xi = \xi_{U,D} = \xi'_{U,D}$, the fermion mixing angles appearing in Eq. (7.7) simplify. The decays into heavy fermion pairs

then contribute to the total width as

$$\frac{\Gamma_{\phi \rightarrow \psi \bar{\psi}}}{m_\phi} = \frac{27}{4\pi} |\xi|^2 \approx 0.8 \quad (\text{MCHM}_{5,1,10}) , \quad (7.9)$$

$$\frac{\Gamma_{\phi \rightarrow \psi \bar{\psi}}}{m_\phi} = \frac{54}{5\pi} |\xi|^2 \approx 0.9 \quad (\text{MCHM}_{5,14,10}) , \quad (7.10)$$

$$\frac{\Gamma_{\phi \rightarrow \psi \bar{\psi}}}{m_\phi} = \frac{117}{20\pi} |\xi|^2 \approx 0.7 \quad (\text{MCHM}_{14,14,10}) , \quad (7.11)$$

$$\frac{\Gamma_{\phi \rightarrow \psi \bar{\psi}}}{m_\phi} = \frac{3}{4\pi} |\xi|^2 \approx 0.6 \quad (\text{MCHM}_{5,1}) , \quad (7.12)$$

where ξ (at $\mu = m_\phi$) has been estimated in Sec. 6 for each benchmark scenario. We conclude that when several fermionic decays are open, the global Higgs is in general a broad resonance, unless all such decays occur very near threshold and there is a further kinematic suppression.

8 Conclusions

We investigated the properties of the physical excitations of the global symmetry breaking vacuum in composite Higgs models. Such a *global Higgs* is expected to interact with the SM Higgs and electroweak gauge bosons, with the SM fermions proportionally to their mass, and with the heavy fermion and vector resonances of the theory. An effective coupling to photons, gluons and transverse electroweak gauge bosons via loops of the resonances is also expected.

We studied in detail the minimal $SO(5)/SO(4)$ case through a general 2-sites model Lagrangian, and found that the dominant interactions of the global Higgs with the SM particles are controlled by two real-valued parameters and by a few group theoretical factors. The couplings of the global Higgs to the SM fermions depend on the global Higgs decay constant \hat{f} and on whether the proto-Yukawa structure is linear or bilinear in Φ , the $SO(5)$ multiplet containing the global Higgs. The couplings of the global Higgs to the pNGBs depend on \hat{f} , on the usual NGB decay constant f , and on the global symmetry group. In a large region of parameter space, the dominant decay modes of the global Higgs are the tree-level decays to the SM Higgs, electroweak gauge bosons, and top quark.

The global Higgs also couples to the (possibly many) fermion resonances that partner with the SM fermions. We analyzed various typical realizations of the $SO(5)$ fermionic sector, with a global Higgs arising either from the **5** or **14** of $SO(5)$. We computed the beta functions of the composite sector, *i.e.* the global Higgs quartic and the $SO(5)$ Yukawa couplings. Evolving these couplings from the strong coupling scale down to the global Higgs mass scale provides a consistent picture of the composite sector, necessary for the analysis of the global Higgs properties.

Loops of fermion and vector resonances of the coset induce an effective coupling of the global Higgs to SM gauge bosons. This is similar to the case of the Higgs-photon coupling induced by top quark and W loops, except that for the global Higgs the fermion multiplicity can be much larger, enhancing the loop amplitude accordingly. We derived

compact formulas for these effective couplings in each realization of the fermion sector in the benchmark models considered.

When several heavy fermion channels are open, the global Higgs is in general a broad resonance. On the other hand, when the decay of the global Higgs into fermion resonances is kinematically suppressed or forbidden, its decay width ranges from $\Gamma_{\text{tot}}/m_\phi \sim 10^{-3}$ to ~ 0.1 , depending on the global Higgs mass and quartic coupling. The global Higgs can thus behave either as a narrow or a broad resonance. In this latter more predictive case, we provided the branching fractions of the global Higgs for each benchmark model.

Although the present study is mostly theoretical, it turns out that the properties of the global Higgs are such that it could in principle be detected at a collider like the LHC. That is, the theoretical aspects of composite Higgs models we explored here may turn into a new way of searching for Higgs compositeness at the LHC. A detailed study of the collider implications of a global Higgs is presented in Ref [21]. As a motivation, we simply observe that the coupling of the global Higgs to gluons, induced by the many fermion resonances of the theory, may be sizeable enough to allow for the production of the global Higgs by gluon fusion at the LHC with 300 fb^{-1} integrated luminosity.

Acknowledgments

This work was supported by the São Paulo Research Foundation (FAPESP) under grants #2011/11973 and #2014/21477-2. E.P. and R.R. were partially funded by a CNPq research grant.

A The Global Higgs in the 14 Representation of $SO(5)$

In Sec. 3 and below, we have assumed that the global Higgs is embedded in a fundamental $\Phi = \mathbf{5}$ of $SO(5)$, *i.e.* it is identified with the $SO(4)$ singlet in the decomposition

$$\mathbf{5} \rightarrow (\mathbf{2}, \mathbf{2}) + (\mathbf{1}, \mathbf{1}). \quad (\text{A.1})$$

We parametrized this decomposition by the NGB matrix U_5 and the radial direction \mathcal{H} as

$$\Phi = U_5 \mathcal{H}, \quad (\text{A.2})$$

and aligned \mathcal{H} as

$$\mathcal{H} = (\hat{f} + \phi)e_5, \quad e_5 = (0, 0, 0, 0, 1)^T. \quad (\text{A.3})$$

This is the most minimal scenario possible.

The next-to-minimal embedding is in the symmetric traceless $\Psi = \mathbf{14}$ representation. Indeed, the decomposition into $SO(4)$ also contains an $SO(4)$ singlet:

$$\mathbf{14} \rightarrow (\mathbf{3}, \mathbf{3}) + (\mathbf{2}, \mathbf{2}) + (\mathbf{1}, \mathbf{1}) \quad (\text{A.4})$$

which we will be parametrizing as follows:²⁴

$$\Psi = U_5 (\mathcal{H} + \mathcal{H}') U_5^\dagger. \quad (\text{A.5})$$

²⁴Unlike the vacuum induced by a vev in the $\mathbf{5}$, which is unique, the breaking by the $\mathbf{14}$ can also lead to other vacua such as $SO(3) \times SO(2)$. We assume here that there exists a potential that leads to the $SO(4)$ vacuum.

Here \mathcal{H}' denotes the $(\mathbf{3}, \mathbf{3})$

$$\mathcal{H}' = \begin{pmatrix} \phi'_{4 \times 4} \\ 0 \end{pmatrix}, \quad (\text{A.6})$$

with ϕ' traceless symmetric, and leads to (non-NGB) heavy states. The singlet is parametrized as

$$\mathcal{H} = (\hat{f} + \phi)e_{14}, \quad e_{14} = \begin{pmatrix} \frac{1}{2\sqrt{5}} \times 1_{4 \times 4} \\ -\frac{2}{\sqrt{5}} \end{pmatrix}. \quad (\text{A.7})$$

Notice that $\text{Tr } e_{14} = 0$ and $\text{Tr } e_{14}^2 = 1$.

A first comment regards the scalar potential. There are now two independent quartic couplings that are conveniently written as

$$V = \frac{\lambda}{4} (\text{tr } \Psi^2 - \hat{f}^2)^2 + \frac{\lambda'}{4} \left(\frac{13}{5} [\text{tr } \Psi^2]^2 - 4 \text{tr } \Psi^4 \right). \quad (\text{A.8})$$

This potential contains an $SO(4)$ symmetric vacuum $\langle \phi' \rangle = 0$ for $\lambda' > 0$, $\lambda > 0$ with

$$m_1^2 = 2\lambda\hat{f}^2, \quad m_9^2 = 2\lambda'\hat{f}^2. \quad (\text{A.9})$$

We will assume that λ' is sufficiently large so as to decouple the nonet near the cutoff.

A second modification concerns the vector resonances. Eq. (3.5) is then still valid provided we use the corresponding covariant derivative

$$\nabla \mathcal{H} = \partial_\mu \mathcal{H} - i \mathcal{A}_\mu^{\hat{a}} [T^{\hat{a}}, \mathcal{H}], \quad (\text{A.10})$$

such that Eq. (3.7) gets modified according to

$$\begin{aligned} & \frac{1}{2} |\nabla \mathcal{H}|^2 + \frac{1}{4} f_\rho^2 \left(\mathcal{A}_\mu^A - i [U_5^\dagger D_\mu U_5]^A \right)^2 \\ &= \frac{1}{2} (\partial_\mu \phi)^2 + \frac{5}{8} (\hat{f} + \phi)^2 (\mathcal{A}_\mu^{\hat{a}})^2 + \frac{f_\rho^2}{4} \left(\mathcal{A}_\mu^{\hat{a}} + \frac{\sqrt{2}}{f} D_\mu h^{\hat{a}} \right)^2 + \dots \end{aligned} \quad (\text{A.11})$$

Proceeding similarly to Eq. (3.7) one obtains

$$\mathcal{L} = \frac{1}{2} (\partial_\mu \phi)^2 + \frac{1}{2} (D_\mu h^{\hat{a}})^2 + \frac{f_\rho^2 \hat{f}^2}{4Z f^2} (\mathcal{B}_\mu^{\hat{a}})^2 + \frac{1}{Z} \left(\frac{1}{2} \hat{f} \phi + \frac{1}{4} \phi^2 \right) \left(\mathcal{B}_\mu^{\hat{a}} - \frac{\sqrt{2} Z f}{\hat{f}^2} D_\mu h^{\hat{a}} \right)^2, \quad (\text{A.12})$$

with $Z = \frac{2}{5}$ and

$$f^{-2} = Z \hat{f}^{-2} + f_\rho^{-2}. \quad (\text{A.13})$$

We will define

$$r_v \equiv \frac{m_\rho^2}{m_a^2} = \frac{Z f^2}{\hat{f}^2} \leq 1, \quad (\text{A.14})$$

yielding

$$\mathcal{L} = \frac{1}{2} (\partial_\mu \phi)^2 + \frac{1}{2} (D_\mu h^{\hat{a}})^2 + \frac{m_a^2}{2g_\rho^2} (\mathcal{B}_\mu^{\hat{a}})^2 + \left(\frac{\phi}{\hat{f}} + \frac{1}{2} \frac{\phi^2}{\hat{f}^2} \right) \left(\frac{\sqrt{m_a^2 - m_\rho^2}}{g_\rho} \mathcal{B}_\mu^{\hat{a}} - \sqrt{r_v} D_\mu h^{\hat{a}} \right)^2, \quad (\text{A.15})$$

as in the case of the $\mathbf{5}$ representation.

B Yukawa Structures

In this appendix we setup the conventions necessary to derive the individual Yukawa couplings, in particular the weights in Tables 2 and 3. The $SO(5)$ fields are parametrized as ($i = 1\dots 4$, $j = 1\dots 6$, $k = 1\dots 9$)

$$\begin{aligned} F &= f_i e_{(4)}^i + s e_{(1)} , \\ A &= a_j \alpha_{(6)}^j + f_i \alpha_{(4)}^i , \\ B &= b_k \beta_{(9)}^k + f_i \beta_{(4)}^i + s \beta_{(1)} , \end{aligned} \tag{B.1}$$

where the e 's are unit vectors, and the α 's (β 's) are antisymmetric (symmetric traceless) orthogonal matrices that are normalized as $\text{tr } \alpha^2 = 1$ and $\text{tr } \beta^2 = 1$. Here we only need the explicit forms of:

$$\begin{aligned} (\beta_{(1)})_{ab} &= \frac{1}{2\sqrt{5}}\delta_{ab} - \frac{2}{\sqrt{5}}\delta_{a5}\delta_{b5} , \\ (\alpha_{(4)}^i)_{ab} &= \frac{1}{\sqrt{2}}(\delta_{ia}\delta_{b5} - \delta_{a5}\delta_{ib}) , \\ (\beta_{(4)}^i)_{ab} &= \frac{1}{\sqrt{2}}(\delta_{ia}\delta_{b5} + \delta_{a5}\delta_{ib}) . \end{aligned} \tag{B.2}$$

With these conventions, kinetic terms are canonically normalized when written as traces. The $SO(5)$ Yukawa couplings are normalized as

$$\mathcal{L} = -\xi \Phi_i (\bar{F}_i P_R S + \bar{F}_j P_R B_{ij} + \bar{F}_j P_R A_{ij}) - \xi \Psi_{ij} (B_{jk} P_R B'_{ki} + B_{jk} P_R A_{ki}) + h.c. \tag{B.3}$$

The $SO(4)$ Yukawas are normalized as

$$\mathcal{L} = -\xi \phi (\bar{b}_k P_R b'_k + \bar{a}_j P_R a'_j + \bar{f}_i P_R f'_i + \bar{s} P_R s') + h.c. \tag{B.4}$$

By comparison, one obtains the weights given in Table 2 and 3.

C Loop Functions

For completeness, we collect here the well-known loop functions (see [28], for example) that appear at 1-loop order when considering the couplings of a scalar to gauge bosons via heavy fermion or spin-1 loops:

$$A_{1/2}(\tau) = 2[\tau + (\tau - 1)f(\tau)]\tau^{-2} , \tag{C.1}$$

$$A_1(\tau) = -[2\tau^2 + 3\tau + 3(2\tau - 1)f(\tau)]\tau^{-2} , \tag{C.2}$$

where

$$f(\tau) = \begin{cases} \arcsin^2 \sqrt{\tau} & \tau \leq 1 \\ -\frac{1}{4} \left[\log \frac{1+\sqrt{1-\tau^{-1}}}{1-\sqrt{1-\tau^{-1}}} - i\pi \right]^2 & \tau > 1 \end{cases} . \tag{C.3}$$

In the limit that $\tau \rightarrow 0$, $A_{1/2}(\tau) \rightarrow 4/3$ and $A_1(\tau) \rightarrow -7$.

References

- [1] G. Panico and A. Wulzer, *The Composite Nambu-Goldstone Higgs*, *Lect. Notes Phys.* **913** (2016) pp.1–316, [[arXiv:1506.01961](#)].
- [2] D. Buttazzo, F. Sala, and A. Tesi, *Singlet-like Higgs bosons at present and future colliders*, *JHEP* **11** (2015) 158, [[arXiv:1505.05488](#)].
- [3] F. Feruglio, B. Gavela, K. Kanshin, P. A. N. Machado, S. Rigolin, and S. Saa, *The minimal linear sigma model for the Goldstone Higgs*, *JHEP* **06** (2016) 038, [[arXiv:1603.05668](#)].
- [4] G. von Gersdorff, E. Pontón, and R. Rosenfeld, *The Dynamical Composite Higgs*, *JHEP* **06** (2015) 119, [[arXiv:1502.07340](#)].
- [5] H. Terazawa, K. Akama, and Y. Chikashige, *Unified Model of the Nambu-Jona-Lasinio Type for All Elementary Particle Forces*, *Phys. Rev.* **D15** (1977) 480.
- [6] W. A. Bardeen, C. T. Hill, and M. Lindner, *Minimal Dynamical Symmetry Breaking of the Standard Model*, *Phys. Rev.* **D41** (1990) 1647.
- [7] R. Contino, L. Da Rold, and A. Pomarol, *Light custodians in natural composite Higgs models*, *Phys. Rev.* **D75** (2007) 055014, [[hep-ph/0612048](#)].
- [8] R. Contino and G. Servant, *Discovering the top partners at the LHC using same-sign dilepton final states*, *JHEP* **06** (2008) 026, [[arXiv:0801.1679](#)].
- [9] J. A. Aguilar-Saavedra, *Identifying top partners at LHC*, *JHEP* **11** (2009) 030, [[arXiv:0907.3155](#)].
- [10] J. Mrazek and A. Wulzer, *A Strong Sector at the LHC: Top Partners in Same-Sign Dileptons*, *Phys. Rev.* **D81** (2010) 075006, [[arXiv:0909.3977](#)].
- [11] A. De Simone, O. Matsedonskyi, R. Rattazzi, and A. Wulzer, *A First Top Partner Hunter’s Guide*, *JHEP* **04** (2013) 004, [[arXiv:1211.5663](#)].
- [12] M. Carena, L. Da Rold, and E. Pontón, *Minimal Composite Higgs Models at the LHC*, *JHEP* **06** (2014) 159, [[arXiv:1402.2987](#)].
- [13] O. Matsedonskyi, G. Panico, and A. Wulzer, *Top Partners Searches and Composite Higgs Models*, *JHEP* **04** (2016) 003, [[arXiv:1512.04356](#)].
- [14] J. Berger, J. Hubisz, and M. Perelstein, *A Fermionic Top Partner: Naturalness and the LHC*, *JHEP* **07** (2012) 016, [[arXiv:1205.0013](#)].
- [15] Y. Okada and L. Panizzi, *LHC signatures of vector-like quarks*, *Adv. High Energy Phys.* **2013** (2013) 364936, [[arXiv:1207.5607](#)].
- [16] G. Cacciapaglia, A. Deandrea, L. Panizzi, S. Perries, and V. Sordini, *Heavy Vector-like quark with charge 5/3 at the LHC*, *JHEP* **03** (2013) 004, [[arXiv:1211.4034](#)].
- [17] J. Kearney, A. Pierce, and J. Thaler, *Exotic Top Partners and Little Higgs*, *JHEP* **10** (2013) 230, [[arXiv:1306.4314](#)].
- [18] A. Angelescu, A. Djouadi, and G. Moreau, *Vector-like top/bottom quark partners and Higgs physics at the LHC*, *Eur. Phys. J.* **C76** (2016), no. 2 99, [[arXiv:1510.07527](#)].
- [19] D. B. Kaplan, *Flavor at SSC energies: A New mechanism for dynamically generated fermion masses*, *Nucl. Phys.* **B365** (1991) 259–278.
- [20] M. Bando, T. Kugo, and K. Yamawaki, *Nonlinear Realization and Hidden Local Symmetries*, *Phys. Rept.* **164** (1988) 217–314.

- [21] S. Fichet, G. von Gersdorff, E. Ponton, and R. Rosenfeld, *The Global Higgs as a Signal for Compositeness at the LHC*, [arXiv:1608.01995](#).
- [22] A. Azatov, R. Contino, A. Di Iura, and J. Galloway, *New Prospects for Higgs Compositeness in $h \rightarrow Z\gamma$* , *Phys. Rev.* **D88** (2013), no. 7 075019, [[arXiv:1308.2676](#)].
- [23] **ATLAS Collaboration**, *Measurements of the properties of the Higgs-like boson in the four lepton decay channel with the ATLAS detector using 25 fb1 of proton-proton collision data*, Tech. Rep. ATLAS-CONF-2013-013, CERN, Geneva, Mar, 2013.
- [24] **ATLAS Collaboration**, M. Aaboud et al., *Searches for heavy diboson resonances in pp collisions at $\sqrt{s} = 13$ TeV with the ATLAS detector*, [arXiv:1606.04833](#).
- [25] **CMS Collaboration**, *Search for massive resonances decaying into pairs of boosted W and Z bosons at $\sqrt{s} = 13$ TeV*, .
- [26] **ATLAS Collaboration**, *Search for resonances decaying to photon pairs in 3.2 fb^{-1} of pp collisions at $\sqrt{s} = 13$ TeV with the ATLAS detector*, .
- [27] **CMS Collaboration**, *Search for new physics in high mass diphoton events in proton-proton collisions at 13TeV*, .
- [28] A. Djouadi, *The Anatomy of electro-weak symmetry breaking. I: The Higgs boson in the standard model*, *Phys. Rept.* **457** (2008) 1–216, [[hep-ph/0503172](#)].